

04
Silicon ablation in air by mono- and bichromatic laser pulses with wavelength 355 and 532 nm

© A.N. Chumakov, V.V. Luchkouski, I.S. Nikonchuk, A.S. Matsukovich

Stepanov Institute of Physics, Belarusian Academy of Sciences, Minsk, Belarus
e-mail: a.chumakov@dragon.bas-net.by

Received July 2, 2021

Revised September 3, 2021

Accepted September 8, 2021

Ablation of silicon sample in air under irradiance of single and double laser pulses with wavelengths 355 and 532 nm was studied by means of optical and scanning electron microscopy, raman spectroscopy, profilometry of laser craters as well as video registration of plasma's plume radiation in time. Dependence of specific sample's material removal on laser fluence and time interval between coupled pulses of bichromatic laser irradiance was established. Spallation of silicon was found in broad range of irradiance parameters and parameters of craters formed by ablation and spallation under the action of bichromatic laser radiation were determined.

Keywords: nanosecond laser ablation, specific mass removal, surface modification, laser plasma dynamics, crater formation, spallation

DOI: 10.21883/TP.2022.01.52527.202-21

Introduction

Owing to the continued progress in laser technology and its engineering applications and to the complexity and nonlinearity of accompanying processes, studies into the interaction of laser radiation with materials and near-surface plasma have remained topical for several decades [1–4]. Various engineering applications of lasers involve laser ablation of materials (i.e., removal of matter of the sample subjected to laser irradiation with a sufficiently high power density that ensures local destruction of the irradiated material with the formation of near-surface plasma and removal of fine material particles). Ablation and removal of material from the irradiated sample surface in air normally grow more intense as the power density of radiation increases and the duration of laser pulses decreases. This continues up to the point when the forming near-surface plasma starts screening markedly the target from laser radiation. The efficiency of laser ablation depends on the optical and thermophysical characteristics of the irradiated material, the wavelength and the power density of laser radiation, and the duration of laser pulses [1–4].

Since silicon is used widely in microelectronics, laser treatment of silicon wafers has been studied extensively in recent years to determine efficient treatment regimes. The absorption coefficient of silicon increases by three orders of magnitude as the irradiation wavelength decreases from 1064 to 266 nm. Therefore, laser treatment of silicon may be made more efficient if one uses the 2nd, 3rd, or 4th harmonics of radiation of a Nd:YAG laser [5–8].

In the case of nanosecond laser irradiation (with a wavelength of 266 nm) of silicon in air, the electron number density and the temperature of plasma and the removal of mass grew evenly as the radiation power density increased from 1 to 20 GW/cm² [5]. However, the crater volume and

the rate of ejection of particles increased sharply as the power density of laser radiation (LR) crossed the threshold of 22 GW/cm². In addition, the growth of the electron number density and the temperature of plasma was slowed down dramatically above the indicated threshold. This suggested explosive boiling as the probable mechanism of mass removal triggered by the transition of superheated silicon from the liquid metal state to the state of a liquid dielectric, which is more transparent to laser radiation [5,6].

Nd:YAG lasers with diode pumping allow one to raise the repetition frequency of laser pulses to several hundred kHz, thus speeding up greatly the process of silicon ablation [7,8], facilitating the production and heating of ablation plasma, and minimizing the production of plasma in air surrounding the irradiated sample [9].

Oxidation, amorphization, recrystallization, evaporation, ablation, and periodic structure formation were observed in experiments on femtosecond laser treatment (at an LR wavelength of ~ 800 nm) of silicon with an increasing radiation power density. It was demonstrated that a threshold power density of ~ 0.2 J/cm², which depends only weakly on the duration and number of laser pulses, is needed in these conditions to achieve silicon ablation [10].

The methods of automated laser treatment of silicon are typically based on ablation under the influence of pulse-periodic laser radiation with high repetition frequency of laser pulses (from 50 to 200 kHz) and high ellipticity of the irradiation spot (in the case of cutting) [7,8,10–12]. The process of stealth dicing is often used to enhance the efficiency of silicon wafer dicing. It involves the formation of a crack along the trajectory of scanning by a laser beam focused sharply onto the sample with rapid local heating of the material due to the exponential growth of the coefficient

of LR absorption and subsequent shock cooling by a coolant jet [13–15].

The use of coupled LR pulses (especially those that differ in wavelength) with an adjustable time interval and sequence order should provide an opportunity to enhance considerably the efficiency of ablation of materials, heating of ablation plasma, and generation of shock waves [9,16,17].

Double-pulse bichromatic laser treatment offers more degrees of freedom for control over the process of laser ablation of materials differing in their thermophysical and optical characteristics. However, it still remains understudied. The aim of the present study is to determine the specific features of laser ablation of silicon in atmospheric air irradiated with nanosecond monochromatic and bichromatic (355 and 532 nm) LR pulses in a wide range of parameters and identify the regimes of efficient specific mass removal and production of near-surface plasma.

1. Experimental setup and measurement techniques

The setup was constructed based on two Nd:YAG lasers LH–2132 and LH–2137 (OOO „LOTIS TII“, Minsk) and a synchronization system for generation of paired nanosecond LR pulses with wavelengths of 355 and 532 nm and durations of 18 and 15 ns, respectively. The sequence order and the time interval between pulses could be adjusted. The time profile of LR pulses was measured with a 11HSP-V2 (Standa) photodetector and a Teledyne Lecroy Wave Surfer 510R oscilloscope with a bandwidth of 1 GHz. The energy of laser pulses was monitored using an Ophir instrument with a PE25BF-DIF-V2 ROHS measurement probe. A coaxial beam of radiation of both lasers was formed using a spectrum splitter and focused with an achromatic lens ($f = 150$ mm) on the surface of a silicon wafer. The targets were (111) silicon wafers with a thickness of 180–375 μm .

The diameter of spots of laser irradiation on the target was 200 μm for $\lambda = 355$ nm and 250 μm for $\lambda = 532$ nm. The maximum possible levels of laser pumping and the attenuation of energy of laser pulses by calibrated radiation filters were used to enhance the uniformity of irradiation spots. The influence of single-pulse monochromatic radiation was studied within the intensity interval of 0.1–5 GW/cm^2 .

The surface of irradiated samples was examined with a TESCAN VEGA 3 (TESCAN, Czech Republic) scanning electron microscope and a multifunctional complex „NanoFlex“ (Solar LS, Republic of Belarus) based on a microscope for excitation and measurement of Raman spectra with LR with a wavelength of 488 nm focused to a spot 100 μm in diameter.

The ablation laser plume was recorded with a video camera [18] featuring an ICX415AL CCD sensor and an I-90U 4/75 lens ($f = 75$ mm). The video camera was operated in the mode of recording of a series of 40 frames with an exposure of ~ 3 ms per frame. The

frames were captured on a signal from the synchronization system based on a G5-54 pulse generator connected to the laser. This allowed us to monitor, to a certain extent, the temporal dynamics of evolution of the plasma plume. The time interval between the laser pulse and the camera synchronization pulse was monitored by the oscilloscope in accordance with signals from the photosensitive diode and the pulse generator, respectively.

The specific mass removal was determined experimentally based on the volume of a through hole in a silicon wafer with a thickness of 180 μm , which was made by a countable number of laser pulses, with the known density of silicon (2.33 g/cm^3) and the measured total energy of laser pulses taken into account. In the case of double-pulse bichromatic treatment, the specific mass removal was determined at different time intervals between laser pulses falling within the range from -40 to $+40$ μs (negative intervals correspond to pulse sequences in which the short-wave laser pulse came first). The following power densities at the irradiation spot were chosen based on research data: $q_{355} = 1.9$ and $q_{532} = 3.5$ GW/cm^2 .

The profiles of laser craters on the surface of silicon were measured with an ACCRETECH Surfcom Crest DX-T profilometer with a resolution of 1 μm .

2. Experimental results and discussion

The irradiation of silicon wafers in air with 10 monochromatic LR pulses with wavelengths of 355 and 532 nm and power densities $q_{355} = 2.16$ and $q_{532} = 4.01$ GW/cm^2 results in the formation of ablation craters with haloes (modification regions) up to 2.5 mm in diameter with a complex structure that is resolved clearly in SEM images (Fig. 1).

Radial „petals“ form in the halo region under the influence of LR with $\lambda = 355$ nm (apparently, due to the recession of microparticles in the process of ablation). Large volumes of molten material solidify at the crater edges, forming a rim. This suggests that a considerable amount of material is melted down during ablation and washed out from the crater. The crater profile is stepped. The formation of microcracks in the halo region (Fig. 1, *a*) should also be noted.

A round crater with an annular rim forms in the process of LR treatment with $\lambda = 532$ nm. The crater halo outside the silicon ablation region is divisible into annular zones formed by the processes of annealing, oxidation, and amorphization on the sample surface (Figs. 1, *c* and 1, *d*).

When silicon is subjected to combined laser irradiation with 10 paired pulses with wavelengths $\lambda = 355$ and 532 nm (interpulse interval $\Delta\tau = -1.4$ μs , $q_{355} = 2.16$ and $q_{532} = 3.76$ GW/cm^2), the crater is also round with a halo of annular zones (Fig. 2, *a*) that differ somewhat from the ones observed after irradiation with LR pulses with a wavelength of 532 nm.

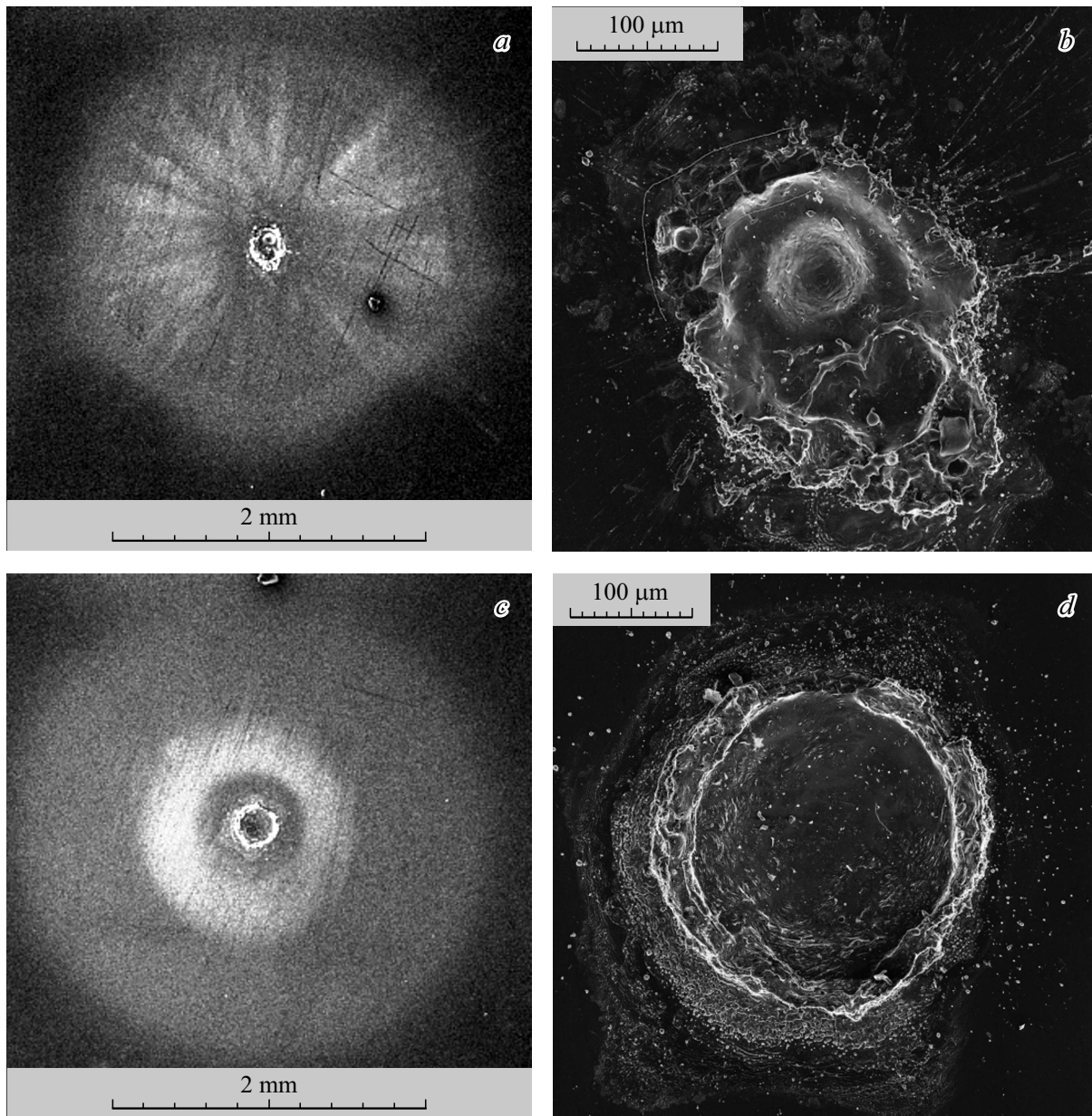


Figure 1. SEM images of silicon samples irradiated with monochromatic LR with a wavelength of 355 (*a, b*) and 532 nm (*c, d*) at radiation power density $q_{355} = 2.16$ and $q_{532} = 4.01$ GW/cm².

It is noteworthy that crystalline silicon is predominant in the crater. This suggests the removal of the greater part of ablation products from the crater. Region 3 with yellow-brown microparticles formed only in the process of irradiation with monochromatic pulses with $\lambda = 355$ nm or paired bichromatic radiation pulses. This may be indicative of the specifics of decay of near-surface plasma formations in these regimes. The amorphous silicon layer is characterized by small thickness. This is evidenced by the dominance of the primary 521 cm^{-1} peak in the Raman spectrum of region 4. The formation of the amorphous silicon layer may be attributed to condensation in the expanding near-surface plasma formation.

The results of video imaging of the temporal evolution of a plasma plume on exposure of silicon to a series of monochromatic LR pulses (355 and 532 nm) in air are presented in Figs. 3 and 4. It follows from the comparison of individual still images of the plasma plume for the 1st, the 15th, and the 25th laser pulses of the series that the production of plasma on exposure to laser pulses with a wavelength of 355 nm is accompanied by intense ejection of particles of the condensed phase into a decreasing solid angle (due to the rapid deepening of the crater with increasing number of irradiating pulses, see Fig. 3, *a*).

In the case of irradiation with laser pulses with a wavelength of 532 nm, the shape of the plasma plume

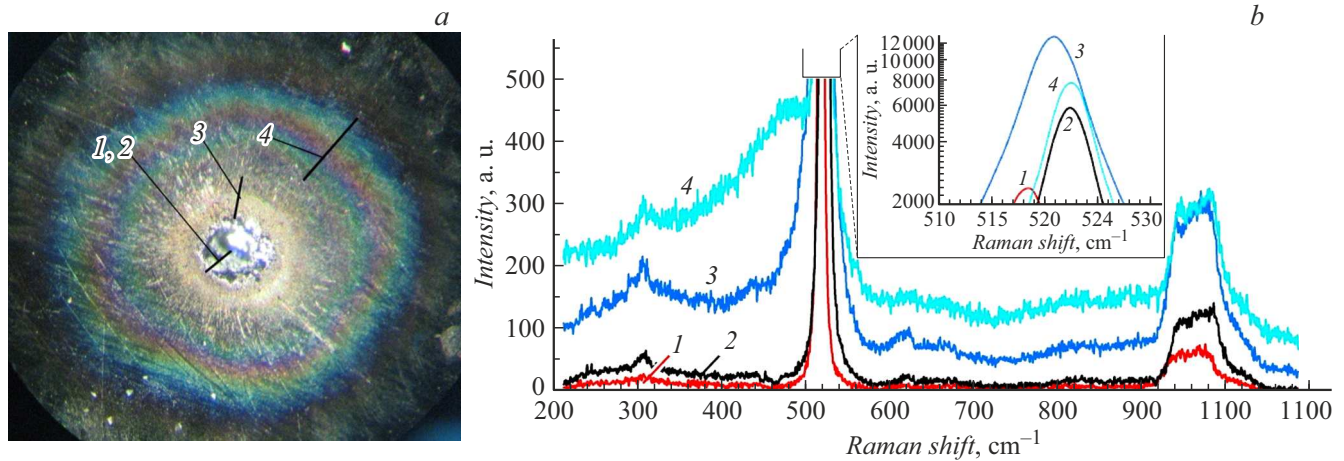


Figure 2. Photomicrograph of the irradiated silicon sample (*a*) and Raman spectra of different regions near the crater (*b*): 1 — crater center, 2 — crater rim, 3 — region with yellow-brown microparticles, and 4 — region with iridescent coloring (interpulse interval $\Delta\tau = -1.4\mu\text{s}$, $q_{355} = 2.16$ and $q_{532} = 3.76\text{ GW/cm}^2$).

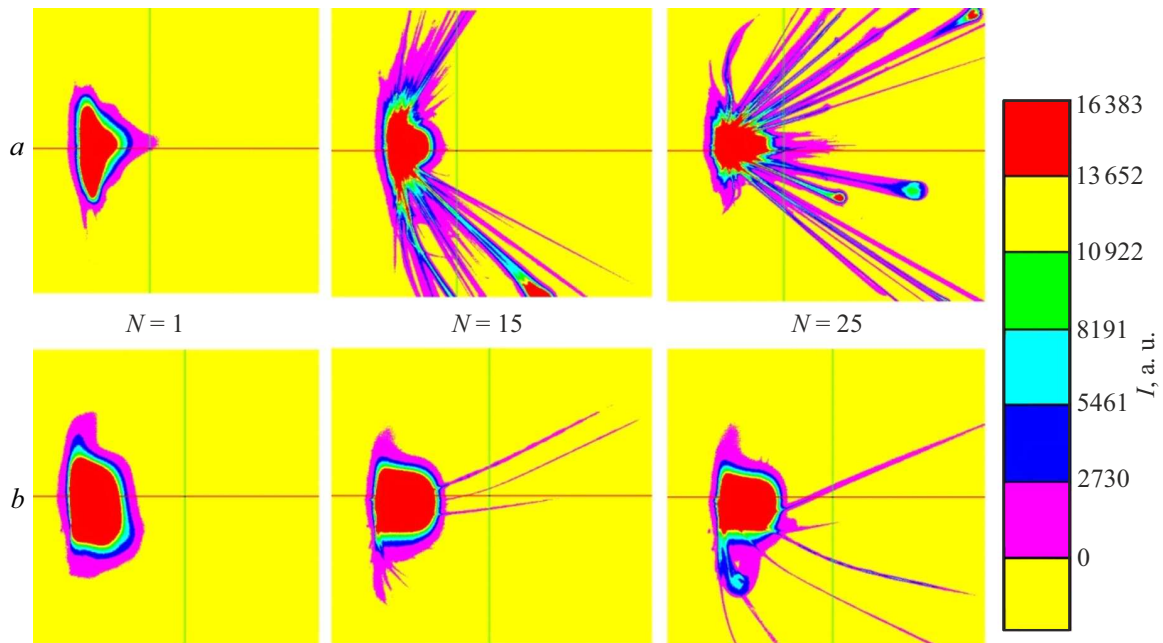


Figure 3. Individual still images of the plasma plume corresponding to the irradiation of silicon in air with the 1st, the 15th, and the 25th laser pulses in a series with a wavelength of 355 (*a*) and 532 nm (*b*). Synchronization pulses were generated before the LR pulse treatment ($\Delta\tau = -4\mu\text{s}$).

remains, on the contrary, virtually unchanged, and the ejection of particles of the condensed phase is marginal and slowly grows in intensity with increasing number of irradiating pulses (Fig. 3, *b*). This suggests that the produced plasma is heated strongly, while the crater depth increases only slightly. Owing to the vertical positioning of irradiated silicon wafers, the tracks of particles tend downward (under the influence of gravity) within a series of irradiating laser pulses. Craters tend to cylindrical and spherical shapes as the number of pulses increases in the process of LR treatment with wavelengths of 355 and 532 nm, respectively.

It follows from the analysis of individual still images of glow of the plasma plume and silicon ablation products with an increasing time delay after irradiation with the 15th laser pulse of the series (Fig. 4) that the plasma plume vanishes after $0.6\mu\text{s}$ in the case of LR treatment with a wavelength of 355 nm, but remains visible for $\sim 23\mu\text{s}$ when the LR wavelength is 532 nm.

The intense ejection of particles of the condensed phase after the 15th laser pulse with a wavelength of 355 nm continues for $\sim 50\mu\text{s}$ (Fig. 4, *a*). In addition, individual particles with their tracks located away from the sample surface are recorded even $280\mu\text{s}$ after laser irradiation.

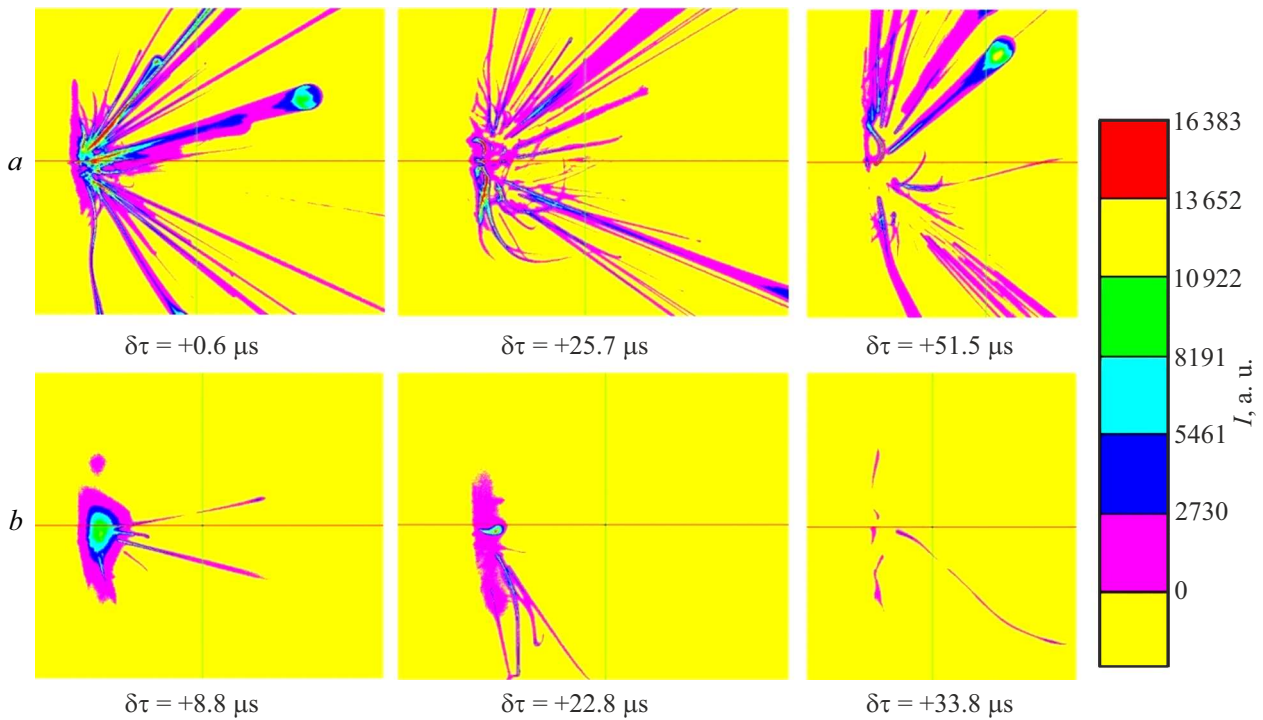


Figure 4. Individual still images of glow of ablation products with an increasing time delay after irradiation of silicon with the 15th laser pulse of a series with a wavelength of 355 (a) and 532 nm (b).

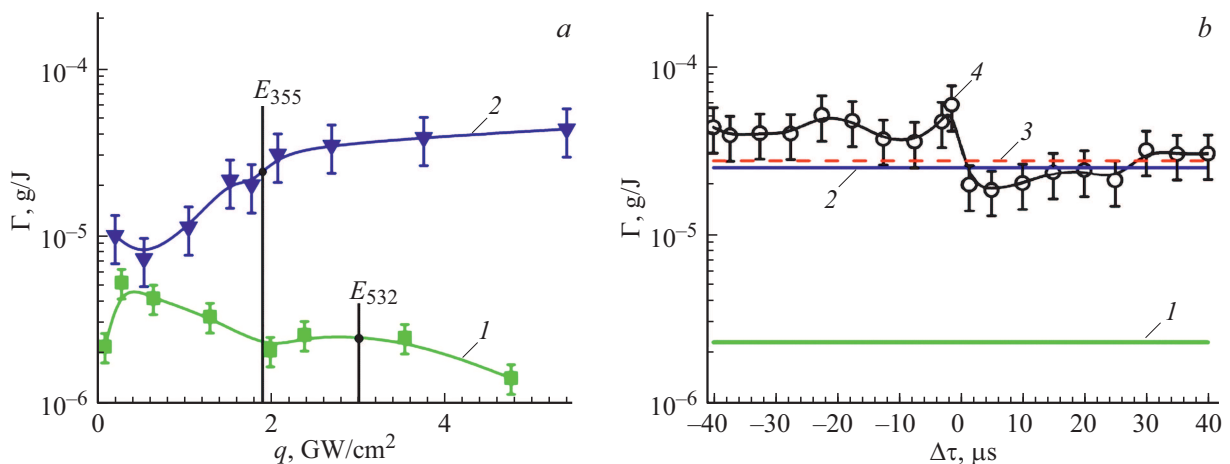


Figure 5. Dependences of the specific mass removal of silicon: a — on the power density of LR with wavelengths of 532 (1) and 355 nm (2); b — on the time interval within bichromatic LR pulses with power density $q_{355} = 1.9$ and $q_{532} = 3.5 \text{ GW/cm}^2$ (1 — $\lambda = 532$, 2 — $\lambda = 355$, 3 — estimate of the overall effect of LR at both wavelengths; 4 — irradiation with bichromatic LR pulses (negative time intervals correspond to pulse sequences in which the 355-nm pulse came first)).

The ejection of particles of the condensed phase after the 15th laser pulse with a wavelength of 532 nm is far less intense (Fig. 4, b). As the plume dies out, the trajectories of particles (tracks) tend downward (under the influence of gravity). Only individual particles are recorded $34 \mu\text{s}$ after irradiation.

The observed differences between the patterns of laser ablation of silicon at the indicated wavelengths are attributable primarily to the manifold growth (by almost 2 orders of

magnitude) of the absorption coefficient of silicon in the irradiated samples occurring as the wavelength of laser irradiation shifts from 532 to 355 nm [7].

In addition, since the coefficient of absorption of laser radiation in the produced plasma depends quadratically on the wavelength, it increases by a factor of two as the irradiation wavelength grows from $\lambda = 355 \text{ nm}$ to $\lambda = 532 \text{ nm}$.

The results of examination of the specific mass removal of silicon in different regimes of monochromatic LR treatment

and irradiation with paired bichromatic radiation pulses with wavelengths of 532 and 355 nm are presented in Fig. 5.

The obtained results revealed the nonlinear nature of dependences of the specific mass removal of silicon on the power density of the irradiating monochromatic LR with wavelengths of 532 and 355 nm within the interval from 0.1 to 5 GW/cm² (Fig. 5, *a*). It should be noted that silicon ablation was observed at the following threshold values of LR power density: $Q_{355} \sim 1.7 \text{ J/cm}^2$ for 355 nm and $Q_{532} \sim 2.5 \text{ J/cm}^2$ for 532 nm. The specific mass removal at an LR wavelength of 532 nm (curve 1 in Fig. 5, *a*) reaches a maximum of $\sim 5 \cdot 10^{-6} \text{ g/J}$ at $q = 0.3 \cdot 10^9 \text{ W/cm}^2$ and undergoes a nonlinear reduction to $\sim 1.5 \cdot 10^{-6} \text{ g/J}$ as the radiation power density increases further to $5 \cdot 10^9 \text{ W/cm}^2$. This is indicative of screening of the irradiated surface by ablation products.

On the contrary, the specific mass removal on exposure to LR with a wavelength of 355 nm (curve 2) drops to a minimum of $\sim 7 \cdot 10^{-6} \text{ g/J}$ at $q = 0.5 \cdot 10^9 \text{ W/cm}^2$, increases sharply to $\sim 4 \cdot 10^{-5} \text{ g/J}$ as the radiation power density grows further to $5 \cdot 10^9 \text{ W/cm}^2$, and reaches saturation at $q = 2.8 \cdot 10^9 \text{ W/cm}^2$. The formation of a through hole in a silicon wafer was characterized by the signs of brittle fracture with spallation of individual fragments on its bottom side.

The identified differences between the dependences of specific mass removal of silicon on the power density of incident radiation at the examined wavelengths correspond to the observed features of dynamics of the plasma plume (Figs. 3 and 4). Specifically, intense ejection of particles of the condensed phase, which continues well after the disintegration of the plasma plume, is observed on exposure of silicon to LR with $\lambda = 355 \text{ nm}$, while LR with $\lambda = 532 \text{ nm}$ produces a glowing plasma plume with weakly pronounced ejection of particles of the condensed phase.

The intense ejection of particles of the condensed phase is likely attributable to the high coefficient of absorption of radiation with a wavelength of 355 nm in silicon. This leads to the formation of a well-pronounced layer of the liquid phase that is removed alongside with the flux of plasma from the irradiated sample surface.

The specific mass removal was also examined under irradiation of silicon in air with paired bichromatic LR pulses with wavelengths of 355 and 532 nm. The dependence of mass removal on the time interval between paired pulses and their sequence order was studied for a number of regimes. A typical dependence of this kind is presented in Fig. 5, *b*. This dependence is also nonlinear. If the short-wave LR pulse came first (i.e., the time interval is negative), specific mass removal 4 is 2–3 times higher than overall removal 3 in the case of monochromatic irradiation at both wavelengths. The maximum values of specific mass removal are achieved at interpulse intervals $\Delta\tau = -20$ and $-1.3 \mu\text{s}$. In the region of positive time intervals between laser pulses, specific mass removal 4 generally remains lower than overall removal 3 and exceeds it somewhat only at intervals from +30 to +40 μs .

Video recording of the plasma plume under bichromatic laser irradiation of silicon was performed in regimes corresponding to the extrema of dependence 4 of the specific mass removal in Fig. 5, *b*. These irradiation regimes corresponded to interpulse time intervals $\Delta\tau = -20, -1.4, +15, +30, +40 \mu\text{s}$. The corresponding video frames were recorded with synchronization from the laser system (Fig. 6).

At $\Delta\tau = -20 \mu\text{s}$, a glowing plume of near-surface plasma and particle tracks are recorded (Fig. 6, *a*) upon arrival of the 2nd laser pulse ($\lambda = 532 \text{ nm}$). The number and the size of particle tracks are significantly smaller than those corresponding to monochromatic irradiation with $\lambda = 355 \text{ nm}$. This may be attributed to the evaporation of a number of particles under the influence of the second pulse of a pair with $\lambda = 532 \text{ nm}$. As the interpulse time interval drops to $\Delta\tau = -1.4 \mu\text{s}$ (Fig. 6, *b*), the brightness and the size of the near-surface plasma plume increase considerably, while the number of particle tracks decreases.

When the sequence order of laser pulses changes (i.e., when time intervals become positive: $\Delta\tau = +15, +30, +40 \mu\text{s}$ (Figs. 6, *c–e*)), the brightness and the size of the near-surface plasma plume decrease, while the number of particle tracks increases appreciably. This is indicative of the fact that the target ablation pattern becomes closer to the one observed under irradiation with monochromatic LR pulses with $\lambda = 355 \text{ nm}$.

The examination of through holes in silicon wafers made by a series of bichromatic LR pulses revealed signs of spallation on the bottom side of the irradiated wafers [22]. Spallation is often studied to obtain data on the strength of materials [23,24]. Spallation of single-crystalline silicon under the influence of nanosecond LR pulses with a wavelength of 355 nm has been examined in [25]. It was demonstrated that the spallation threshold in through-hole drilling depends linearly on the thickness of silicon wafers and is equal to $\sim 6.5 \text{ GW/cm}^2$ for a wafer 225 μm in thickness.

In view of this, ablation craters on the face side of silicon wafers and spallation craters on their bottom side were examined in detail by electron microscopy and profilometry. When a silicon wafer 180 μm in thickness was irradiated with a series of LR pulses with $\lambda = 355 \text{ nm}$ and power density 1.5 GW/cm^2 , spallation on the bottom side of the wafer was initiated after irradiation with ~ 10 pulses even before the formation of a through hole. The indicated LR power density corresponds to the region of a sharp increase in specific mass removal (2) in Fig. 5, *a*.

The parameters of ablation and spallation craters in the regime of bichromatic laser treatment of silicon wafers were studied at radiation power density $q_{355} = 1.9 \text{ GW/cm}^2$ and $q_{532} = 3.5 \text{ GW/cm}^2$ and interpulse time interval $\Delta\tau = -3 \mu\text{s}$ (Fig. 7).

The experiments revealed that two pairs of bichromatic irradiating laser pulses did not induce spallation on the bottom side of the silicon wafer. Spallation in the indicated regime was observed only after irradiation with four or

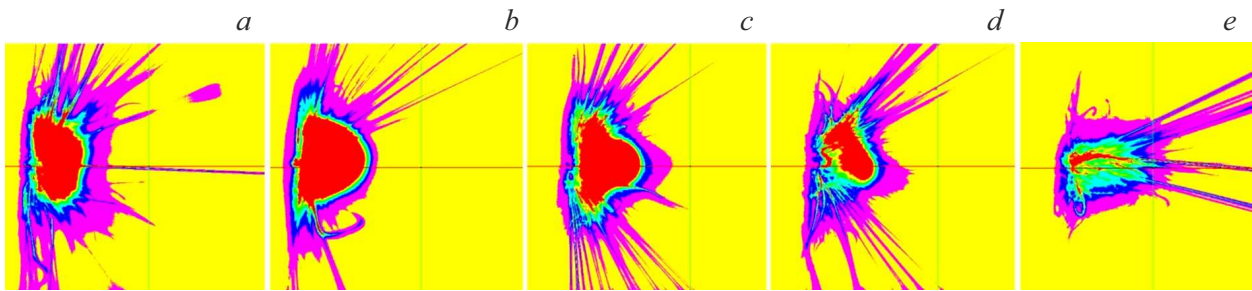


Figure 6. Individual still images of glow of the plasma plume in the case of bichromatic laser treatment ($\lambda = 355, 532 \text{ nm}$) of a silicon wafer with different time intervals and sequence order of pulses: *a* — $\Delta\tau = -20$; *b* — $\Delta\tau = -1.4$; *c* — $\Delta\tau = +15$; *d* — $\Delta\tau = +30$; *e* — $\Delta\tau = +40 \mu\text{s}$ (negative time intervals correspond to pulse sequences in which the 355-nm pulse came first; the start of image capture corresponds to the arrival of the second pulse in a pair).

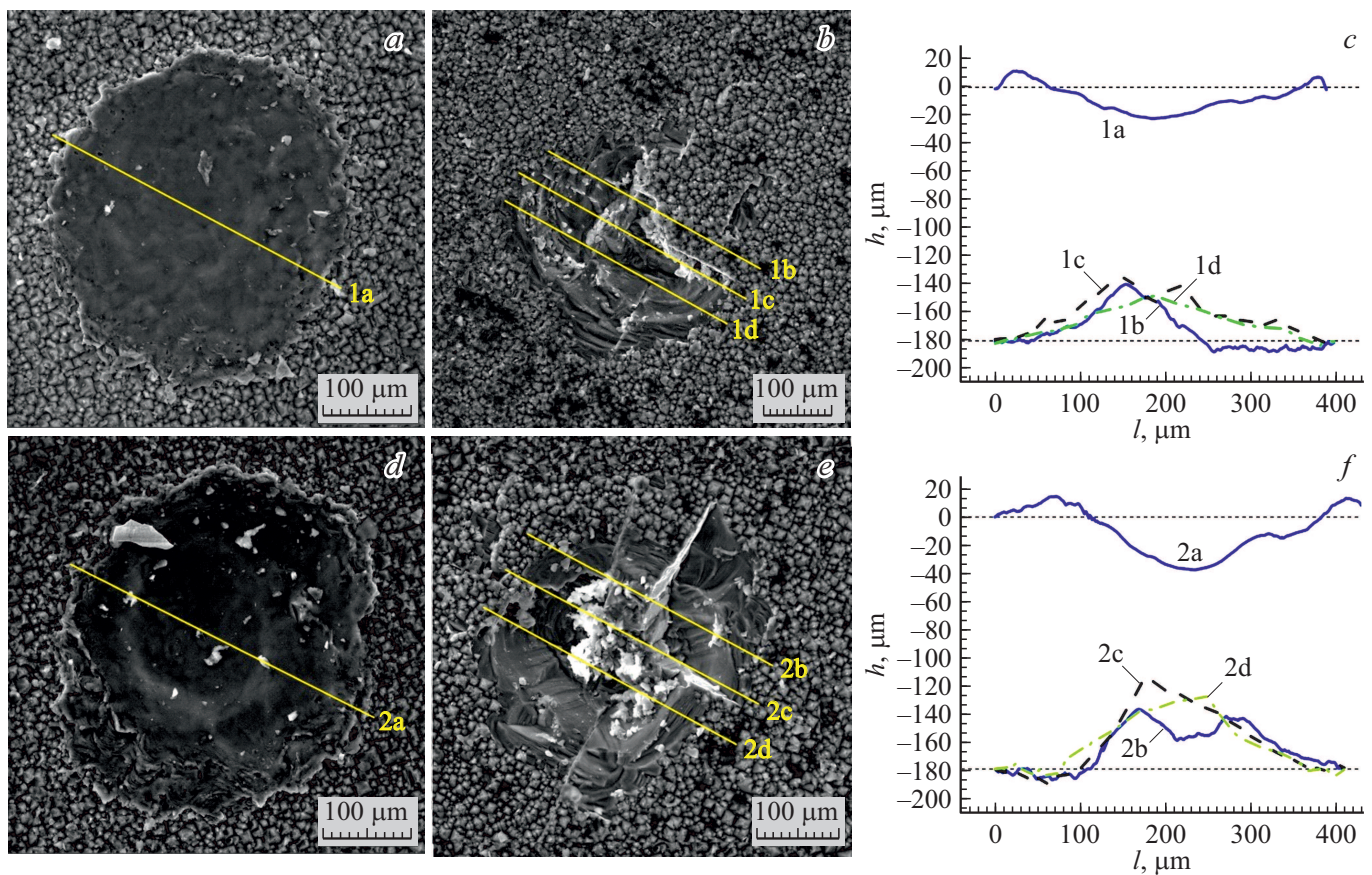


Figure 7. SEM images of ablation (*a, d*) and spallation (*b, e*) craters and the corresponding profiles (*c, f*), formed as a result of irradiation with four (*a–c*) and eight pairs (*d–f*) of LR pulses with wavelengths of 355 and 532 nm (treatment parameters: $q_{355} = 1.9$, $q_{532} = 3.5 \text{ GW/cm}^2$, $\Delta\tau = -3 \mu\text{s}$).

more pairs of bichromatic laser pulses. Typical SEM images of ablation and spallation craters are shown in Fig. 7 for irradiation with four (Figs. 7, *a* and 7, *b*) and eight (Figs. 7, *d* and 7, *e*) pairs of pulses. The results of measurement of their profiles are also presented (Figs. 7, *c* and 7, *f*).

The difference in shape between ablation and spallation craters stands out. The typical shape of ablation craters is that of a sphere segment, while spallation

craters have an irregular shape (formed by several partial spalls) with a roughly triangular profile. It should be noted that the maximum depth of spallation craters is 1.5–2 times higher than the maximum depth of ablation ones. This suggests that spallation produces a significant contribution to the specific mass removal in the process of drilling of through holes in the indicated treatment regimes (Fig. 5, *b*).

Conclusion

Ablation of silicon wafers in air under the influence of monochromatic and bichromatic laser pulses with a power density of 0.1–5.0 GW/cm² and wavelengths of 355 and 532 nm was studied experimentally. It was established that the specific mass removal of silicon grows nonlinearly from $\sim 7 \cdot 10^{-6}$ to $4 \cdot 10^{-5}$ g/J as the power density of laser radiation with a wavelength of 355 nm increases to $5 \cdot 10^9$ W/cm², while the specific mass removal in the case of irradiation at 532 nm decreases nonlinearly from $\sim 5 \cdot 10^{-6}$ g/J (at $q = 0.3 \cdot 10^9$ W/cm²) to $\sim 1.5 \cdot 10^{-6}$ g/J at $q = 5 \cdot 10^9$ W/cm². Video recording data revealed that laser irradiation at 355 nm is accompanied by the formation of a plasma plume with substantial ejection of particles of the condensed disperse phase, while LR with a wavelength of 532 nm induces the formation of a well-developed plasma plume with an insignificant number of particles of the disperse phase. A modification region ~ 2.5 mm in diameter forms around the laser crater on the silicon surface. The structure and the composition of this region depend on the power density and the wavelength of laser radiation and time parameters of laser pulses.

The specific mass removal of silicon was maximized under the influence of paired bichromatic LR pulses with wavelengths of 355 and 532 nm (with the short-wave pulse being the first in a pair) and depended on the radiation power density and the interpulse time interval. The maximum mass removal observed at interpulse intervals $\Delta\tau = -20$ and $-1.3 \mu\text{s}$ exceeded the overall removal in the case of monochromatic irradiation by a factor of 2–3. The most well-developed and bright plasma plume also formed in this regime. This is indicative of its significant heating by the incident laser radiation.

Spallation on the bottom side of a silicon wafer was observed after irradiation with a series of 10–15 LR pulses with a wavelength of 355 nm and a power density of 1.5 GW/cm^2 even before the formation of a through hole in the wafer. The characteristics of ablation and spallation craters formed under irradiation with paired bichromatic LR pulses were determined. It was established that spallation produces a significant contribution to the specific mass removal in the process of drilling of through holes in bichromatic LR treatment regimes.

Funding

This study was supported by the state research program of the Republic of Belarus „Convergence — 2025“ (subprogram „Microworld, Plasma, and the Universe“).

Conflict of interest

The authors declare that they have no conflict of interest.

References

- [1] S.I. Anisimov, Ya.A. Imas, G.S. Romanov, Yu.V. Khodyko, *Deistvie izlucheniya bol'shoi moshchnosti na metally* (Nauka, M., 1970) (in Russian).
- [2] J.F. Ready, *Effects of High-Power Laser Radiation* (Academic Press, 1971).
- [3] W.W. Duley, *Laser Processing and Analysis of Materials* (Springer, Boston, 1983).
- [4] M.N. Libenson, E.B. Yakovlev, G.D. Shandybina, *Vzaimod-eistvie lazernogo izlucheniya s veshchestvom (silovaya optika). Chast' II. Lazernyi nagrev i razrushenie materialov* (NIU ITMO, St. Petersburg, 2014) (in Russian).
- [5] H.C. Liu, X.L. Mao, J.H. Yoo, R.E. Russo. *Spectrochim. Acta, Part B*, **54** (11), 1607 (1999). DOI: 10.1016/S0584-8547(99)00092-0
- [6] J.H. Yoo, S.H. Jeong, R. Greif, R.E. Russo. *J. Appl. Phys.*, **88** (3), 1638 (2000). DOI: 10.1063/1.373865
- [7] M. Panzner, J. Kasper, H. Wust, U. Klotzbach, E. Beyer. *Proc. SPIE*, **4637**, 496 (2002). DOI: 10.1117/12.470659
- [8] H. Pantsar, H. Herfurth, S. Heinemann, P. Laakso, R. Penttila, Y. Liu, G. Newaz. In: *27th International Congress on Applications of Lasers & Electro-Optics* (Temecula California, ALIA, 2008), p. 278. DOI: 10.2351/1.5061387
- [9] L.Ya. Min'ko, A.N. Chumakov, N.A. Bosak, *Sov. J. Quantum Electron.*, **20** (11), 1389 (1990). DOI: 10.1070/QE1990v020n11ABEH007540
- [10] J. Bonse, S. Baudach, J. Krüger, W. Kautek, M. Lenzner. *Appl. Phys. A*, **74**, 19 (2002). DOI: 10.1007/s003390100893
- [11] J.M. Bovatsek, R.S. Patel. *Proc. SPIE*, **7585**, 75850K (2010). DOI: 10.1117/12.845298
- [12] G. Galasso, M. Kaltenbacher, A. Tomaselli, D. Scarpa. *J. Appl. Phys.*, **117** (12), 123101 (2015). DOI: 10.1063/1.4915118
- [13] V.S. Kondratenko, *Sposob rezki khрупkikh materialov*, RF Patent No. 2024441 (1991) (in Russian).
- [14] T. Monodane, E. Ohmura, F. Fukuyo, K. Fukumitsu, H. Morita, Y. Hirata. *JLMN*, **1** (3), 231 (2006). DOI: 10.2961/jlmn.2006.03.0016
- [15] V.S. Kondratenko, A.S. Naumov, *Vestn. MGTU MIREA*, **2** (3(8)), 1 (2015) (in Russian).
- [16] A.N. Chumakov, N.A. Bosak, P.I. Verenich. *High Temp. Mater. Processes*, **18** (4), 269 (2014). DOI: 10.1615/HighTempMatProc.2015015608
- [17] A.N. Chumakov, N.A. Bosak, A.V. Panina. *J. Appl. Spectr.*, **84**, 620 (2017). DOI: 10.1007/s10812-017-0519-y
- [18] I.S. Nikonchuk, A.N. Chumakov. *J. Phys.: Conf. Ser.*, **666**, 012021 (2016). DOI: 10.1088/1742-6596/666/1/012021
- [19] P.G. Spizzirri, J.H. Fang, S. Rubanov, E. Gauja, S. arXiv:1002.2692 [cond-mat.mtrl-sci] (Cornell University, NY.)
- [20] T.P. Nguyen, S. Lefrant. *Solid St. Commun.*, **57** (4), 235 (1986). DOI: 10.1016/0038-1098(86)90146-8
- [21] V.S. Levitskii, Candidate's Dissertation in Engineering (LETI, St. Petersburg, 2016) (in Russian).
- [22] V.V. Lychkovskii, A.N. Chumakov, in *Int. School-Conf. Modern Problems in Physics*, ed. I.S. Nikonchuk, M.S. Usachenok (Inst. Phys. NAS Belarus, Minsk, 2020), pp. 37–38 (in Russian).

- [23] Ya.B. Zel'dovich, Yu.P. Raizer, *Fizika udarnykh voln i vysokotemperaturnykh gidrodinamicheskikh yavlenii* (Nauka, M., 1966) (in Russian).
- [24] S.A. Abrosimov, A.P. Bazhulin, V.V. Voronov, A.A. Geras'kin, I.K. Krasnyuk, P.P. Pashinin, A.Yu. Semenov, I.A. Stuchebryukhov, K.V. Khishchenko, V.E. Fortov. *Quant. Electron.*, **43** (3), 246 (2013).
DOI: 10.1070/QE2013v043n03ABEH015106
- [25] J. Ren, S.S. Orlov, L. Hesselink. *J. Appl. Phys.*, **97**, 104304 (2005). DOI: 10.1063/1.1896095